Infrared Spectroscopic Studies on the Photocatalytic Hydrogenation of Norbornadiene by Group 6 Metal Carbonyls. 2. The Role of the Diene and the Characterization of (η^4-Norbornadiene)(η^2-norbornadiene)$M(CO)_3$ Complexes

P. Michael Hodges, Sarah A. Jackson,[‡] Jürgen Jacke,[§] Martyn Poliakoff,* James J. Turner, and Friedrich-Wilhelm Grevels[§]

Contribution from the Department of Chemistry, University of Nottingham, Nottingham, NG7 2RD England, and the Max Planck Institut für Strahlenchemie, D-4330 Mülheim a.d. Ruhr, Federal Republic of Germany. *Received June 19, 1989*

Abstract: UV laser flash photolysis of $M(CO)_6$ and $(NBD)M(CO)_4$ (NBD = norbornadiene) is used to generate, respectively, the intermediates $M(CO)_5(s)$ (s = *n*-heptane; M = Cr, Mo, and W) and (η^4-NBD)$M(CO)_3$(s) (*fac* and *mer* isomers; M = Mo and W). Fast (μs) time-resolved IR spectroscopy is then used to measure the rates of reaction of these intermediates with species likely to be components of the catalytic hydrogenation mixture (e.g., H_2, NBD, CO, etc.). The measurements show that, for a particular intermediate, the rates of reaction with H_2 and NBD are quite similar. Thus, in a typical catalytic reaction mixture, intermediates are more likely to react with NBD than H_2, because the concentration of NBD is considerably higher than that of H_2. Fourier-transform IR is used to monitor the carbonyl species present in solution during photocatalytic deuteration at room temperature. These include the previously unknown complexes *fac*- and *mer*-(η^4-NBD)(η^2-NBD)$M(CO)_3$. In the case of W, it is shown that accumulation of *mer*-(η^4-NBD)(η^2-NBD)$W(CO)_3$ in the solution frustrates the catalytic deuteration [as monitored by the ν(C-D) IR bands of the deuterated products]. Furthermore, there is a striking wavelength dependence in the catalytic efficiency of the W system. *mer*-(η^4-NBD)(η^2-NBD)$W(CO)_3$ is sufficiently stable for us to have isolated a sample (ca. 90% purity). ^{13}C NMR data support the IR identification of the complex. Liquid Xe is used to generate samples of *fac*-(η^4-NBD)(C_2H_4)$Mo(CO)_3$, which is used as a model for the photochemical behavior of *fac*-(η^4-NBD)(η^2-NBD)$M(CO)_3$. The results of this paper are combined with those of part 1 (preceding paper) to propose an overall scheme for the catalytic hydrogenation. The suggested role of the (η^4-NBD)(η^2-NBD)$M(CO)_3$ compounds in this scheme is to facilitate the *fac* → *mer* isomerization of the (η^4-NBD)$M(CO)_3$ moiety.

This is the second of two papers investigating the mechanism of the hydrogenation of dienes, particularly of norbornadiene (NBD), photocatalyzed by group 6 metal carbonyls. The first

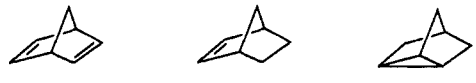

NBD NBN NTC

paper[1] was concerned largely with the role of H_2 in the catalytic process, and although hydrogenation ultimately involves the cleavage of the H-H bond in H_2, we found no evidence for classical dihydride species in this system. However, we did detect a number of species with nonclassical η^2-H_2 and η^4-dienes (or η^2-alkenes) coordinated to the same d^6 metal cluster. These species were identified by IR spectroscopy both in liquid Xe (LXe) solution at −90 °C and in *n*-heptane at room temperature. We suggested that the hydrogenation products nortricyclene (NTC) and norbornene (NBN) were formed, respectively, from the *fac* and *mer* isomers of $(NBD)M(CO)_3(H_2)$ (eqs 1 and 2). (In these equations

(1)

NTC

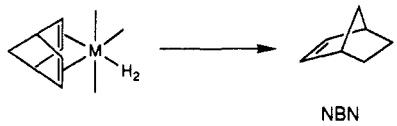

(2)

NBN

and subsequent schemes, carbonyl groups are represented by lines without labels; all other ligands are shown explicitly.) At the same time, we used fast time-resolved IR (TRIR) on a microsecond time scale to identify two intermediates in the photolysis of $(NBD)M(CO)_4$ in *n*-heptane solution. *fac*-$(NBD)M(CO)_3$(*n*-hept) is the major photoproduct and *mer*-$(NBD)M(CO)_3$(*n*-hept) the minor.

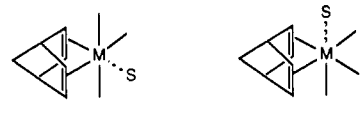

mer fac

This paper is devoted largely to experiments at room temperature and focuses, in particular, on the role of the diene substrate in the catalytic reaction. The diene is important because, initially at least, it is present in much higher concentrations than the other components of the hydrogenation mixture. Typical concentrations might be $M(CO)_6$ (ca. 1×10^{-3} M), diene (0.1 M), and dissolved H_2 ($(3-6) \times 10^{-3}$ M).[2] Hydrogenation is achieved by irradiating such a solution with UV light, usually for several hours (see the Experimental Section for fuller details). Thus, during irradiation, the mixture is quite complex, containing H_2, diene, $M(CO)_6$, diene/carbonyl species, and, in the later stages, hydrogenation products.

Our strategy, therefore, has been to use TRIR to measure the reaction kinetics of intermediates [e.g., $(NBD)M(CO)_3$, etc.] with the individual components of the hydrogenation mixture (e.g., H_2, NBD, etc.). TRIR is a particularly good technique for such measurements because the ν(C-O) IR bands of precursor, intermediate, and product are usually well separated and the individual species can be monitored without any problems of

[‡] Present address: Laboratoire de Chimie Theorique, Universite de Paris Sud, 91405 Orsay Cedex, France.

[§] Max Planck Institut für Strahlenchemie, Mülheim.

(1) Part 1: Jackson, S. A.; Hodges, P. M.; Poliakoff, M.; Turner, J. J.; Grevels, F.-W. *J. Am. Chem. Soc.*, preceding paper in this issue. This paper contains a number of references to earlier work on these hydrogenation reactions, and these are not repeated here.

(2) The solubility of H_2 in hydrocarbon solution is surprisingly low; 15 psi of H_2 (1 atm) will dissolve in cyclohexane to give a 3.8×10^{-3} M solution (Dymond, J. H. *J. Phys. Chem.* **1967**, *71*, 1829. Church, S. P.; Grevels, F.-W.; Hermann, H.; Schaffner, K. *J. Chem. Soc., Chem. Commun.* **1985**, 30).

0002-7863/90/1512-1234$02.50/0

overlapping absorptions. We have then complemented these kinetic results with FTIR spectra of actual hydrogenation mixtures, which were recorded after various periods of UV irradiation.

When D_2 is used instead of H_2, FTIR proves to be an extremely useful noninvasive technique for monitoring the species present in the solution. This approach has an advantage over chromatography (GLC) because one can monitor in a single measurement both the relatively unstable metal carbonyl species, via ν(C–O) bands, and the deuterated products, via ν(C–D) absorptions (2300–2100 cm^{-1}). We also report a new refinement of LXe experiments in which a large excess of ethene is used to generate $(NBD)(C_2H_4)M(CO)_3$ model compounds and is then vented so that the compounds can be studied in "clean" Xe solution.

The TRIR and FTIR experiments presented in this paper reveal that $(\eta^4\text{-NBD})(\eta^2\text{-NBD})M(CO)_3$ compounds play a previously unsuspected role in these hydrogenation systems. In particular, the relative stabilities of $(\eta^4\text{-NBD})(\eta^2\text{-NBD})M(CO)_3$ (M = Cr, Mo, and W) provide a good explanation of why, under some photolysis conditions, $W(CO)_6$ is much less efficient a catalyst for the hydrogenation of NBD than are $Mo(CO)_6$ and $Cr(CO)_6$. We then combine the results of both our papers to propose an overall mechanism for the hydrogenation of NBD.

Experimental Section

(i) **TRIR Measurements.** The apparatus for TRIR (pulsed XeCl UV laser, 308 nm, and CW CO IR laser) was described in the previous paper.[1] All measurements were carried out in *n*-heptane (Aldrich, HPLC grade). This solvent is preferable to cyclohexane, which has a relatively intense IR absorption at ca. 1990 cm^{-1}. Typically, a solution of metal carbonyl (5×10^{-4} M) was made up in *n*-heptane that had been distilled over CaH_2 under an atmosphere of N_2. If required, liquid diene or alkene was added at this stage. The solution, contained in a graduated Pyrex vessel (ca. 150 mL) sealed with a greaseless PTFE tap, was degassed.[3] The vessel was then connected directly to a PTFE flow system.[4] TRIR measurements were made in an evacuable IR cell (CaF_2 windows, 1-mm pathlength). All measurements were carried out under a positive pressure of gas (Messer Griesheim or BOC Research Grade): CO, N_2, H_2 (or Ar when an inert atmosphere was required). The solution was changed between each shot of the UV laser.

Kinetic traces were analyzed on a BBC Master 128 microcomputer with specially written programs. Since each pulse of the UV laser destroys less than 10% of the parent carbonyl, the concentration of all of the primary photoproducts was much lower than that of added reactant, and all traces gave satisfactory pseudo-first-order decays (i.e. plots of ln [absorbance] vs time were linear). For each compound, control measurements were made under an Ar atmosphere and in the absence of added reactants to assess the effect of trace impurities and reaction between intermediates and unphotolyzed starting material.[1,5]

In many experiments, it was possible to monitor not only the decay of the intermediate but also the growth of the corresponding product. The rates of these two processes were in close agreement. In the case of $M(CO)_5$, k_{obs} was much greater in the presence of added ligands than in the presence of Ar, and it is reasonable to calculate bimolecular rate constants, k_2, by dividing the value of k_{obs} by the reagent concentration without correction for the marginal effects of other reaction pathways. By contrast, $(NBD)M(CO)_3$ intermediates decay rapidly even in the absence of added ligands (see preceding paper), and it was necessary to correct[6] for this effect when calculating k_2. In all cases, we present the raw value of k_{obs} as well as calculated value of k_2. In most of our measurements, the overall uncertainty in the bimolecular rate constants should be less than ±10%, but the errors are probably somewhat larger with the $(NBD)M(CO)_3$ intermediates because of the short lifetimes of the intermediates and the corrections for decay in the absence of ligand.[6] In the case of $(NBD)Cr(CO)_4$, the intermediates were so reactive that precise kinetic measurements could not be made on our TRIR apparatus.[5]

(ii) **Room Temperature FTIR Measurements.** Briefly, these experiments involved the prolonged UV photolysis of a hydrocarbon solution of $M(CO)_6$ and a diene, under a pressure of D_2. Small portions of the solution were extracted during photolysis in order to monitor the growth of new products by IR spectroscopy. The deuterated products then have C–D bonds that absorb in a region of the IR spectrum (2300–2100 cm^{-1}) well away from the absorptions of hydrocarbon solvents.[7] It has been noted[8] previously that there are differences in the product yield between experiments with H_2 and D_2 but these differences are not important here as the ν(C–D) bands are not analyzed quantitatively.

For these experiments the basic technique of solution preparation was the same as described above for TRIR. A small amount (ca. 20 mL) of a solution of $M(CO)_6$ (ca. 1×10^{-3} M) and diene (0.1 M) was placed in a Pyrex tube (volume ca. 150 mL) fitted with a greaseless tap. The solution was degassed and ca. 25 psi of D_2 was admitted. Butadiene, which is gaseous at room temperature, was added after degassing the solvent and before the introduction of D_2 (in these cases D_2 was added to give a total pressure of 25 psi). Three lamps were used for photolysis; a 250-W high-pressure Hg arc, a medium-pressure Hg arc (Philips HPK 125 W with or without soda glass filter, >320 nm), and a Wotan Vitalux 300-W sunlamp. During photolysis the tube was shaken continuously to maximize the contact between gas and solution. All photolyses were carried out in the same Pyrex vessel.

At intervals, samples of the solution were taken for FTIR analysis by inverting the tube (i.e., with the tap at the bottom) and briefly opening the tap. The gas pressure forced out a small amount of solution without venting the gas. IR spectra were recorded with a Nicolet MX-3600 FTIR interferometer (32 K data points, 2-cm^{-1} resolution) and, usually, were the average of 100 scans. For anaerobic conditions, the solution was sampled with a flow system similar to that used for TRIR.[4]

(iii) **Generation of Ethene Complexes in Liquid Xenon.** The experimental details for using liquefied xenon (LXe) were given in our first paper. Here we outline a new technique for the preparation of unstable alkene complexes in LXe. Alkenes are generally quite soluble in LXe, and because of the long pathlength (2.5 cm) of our cell, large sections of the IR spectrum can be masked by the absorptions of the alkene. For this reason, previous LXe experiments have generally used rather low concentrations of alkene and computer subtraction to improve spectral quality.[9]

Our new technique exploits the fact that ethene is very volatile compared to carbonyl complexes. We use a relatively large amount of ethene in our cell (ca. 20 psi pressure in the uncooled cell). Under these conditions, combination and overtone bands of the dissolved C_2H_4 obscure virtually all of the ν(C–O) region (and many other parts) of the IR spectrum. Two small windows occur between 2100 and 1800 cm^{-1}, which are just sufficient to monitor the growth of photolysis products. After UV photolysis of the dissolved carbonyl complex, all of the C_2H_4/LXe mixture is vented while the cell is kept at −90 °C. All the C_2H_4 is pumped away, and after a short period of evacuation (typically 5 min at 7×10^{-5} Torr), fresh xenon is admitted into the cell. The IR spectrum of the photolysis products can now be studied without spectroscopic interference from free C_2H_4.

(iv) **Isolation of *mer*-$(\eta^4\text{-NBD})(\eta^2\text{-NBD})W(CO)_3$.**[10] $(\eta^4\text{-NBD})W(CO)_4$ (0.78 g, 2.0 mmol) and 2.2 mL (1.86 g, 20 mmol) of freshly distilled NBD were dissolved in 200 mL of *n*-pentane. After 45 min of irradiation (Philips HPK 125-W Hg lamp, immersion well apparatus, solidex glass >280 nm) at −30 °C (90% conversion), the solution was filtered, and the volatiles were stripped off at −10 °C. Recrystallization of the oily residue from 40 mL of pentane at dry ice temperature yielded a yellow-brown precipitate, which was recrystallized from 20 mL of pentane. A yellow-brown solid (0.38 g; mp ca. −45 °C) was obtained, containing about 10% $(\eta^4\text{-NBD})W(CO)_4$ impurity as judged by IR. Evaporation of the mother liquor yields a second, rather purer, crop of

(3) The solution was degassed by pumping on the solution at room temperature (the graduations on the vessel allow us to correct for solvent lost through degassing). We have shown previously that rate constants obtained from solutions degassed in this way are the same as those obtained with solutions degassed by the more conventional freeze–thaw technique (Creaven, B. S.; Dixon, A. J.; Kelly, J.; Long, C.; Poliakoff, M. *Organometallics* **1987**, *6*, 2600).

(4) Dixon, A. J.; Healy, M. A.; Hodges, P. M.; Moore, B. D.; Poliakoff, M.; Simpson, M. B.; Turner, J. J.; West, M. A. *J. Chem. Soc., Faraday Trans. 2* **1986**, *82*, 2083. Hodges. P. M. Ph.D. Thesis, University of Nottingham, UK, 1988.

(5) Dobson, G. R.; Hodges, P. M.; Healy, M. A.; Poliakoff, M.; Turner, J. J.; Firth, S.; Asali, K. J. *J. Am. Chem. Soc.* **1987**, *109*, 4218.

(6) These corrections were calculated on the assumption that the overall rate law was of the form $k_{obs} = k_2[L] + k_{Ar}$, where k_2 is the bimolecular rate constant, k_{Ar} is the rate of decay under an Ar atmosphere in the absence of any ligand, and [L] is the concentration of the ligand L. Although this correction clearly affected the absolute values calculated for k_2, the relative values of k_2 for different ligands were only slightly changed. Our overall conclusion as to the relative rates of reaction with H_2 and NBD are not therefore dependent on the validity of the correction.

(7) We have used the detection of ν(C–D) bands on a previous occasion as evidence for the presence of deuterated ethane in LXe (Duckett, S. B.; Haddleton, D. M.; Jackson, S. A.; Perutz, R. N.; Poliakoff, M.; Upmacis, R. K. *Organometallics* **1988**, *7*, 1526).

(8) For a general review of this photocatalytic hydrogenation reaction, see: Moggi, L.; Juris, A.; Sandrini, D.; Manfrin, M. F. *Rev. Chem. Intermed.* **1981**, *4*, 171.

(9) Gadd, G. E.; Poliakoff, M.; Turner, J. J. *Inorg. Chem.* **1986**, *25*, 3604.

(10) Jacke, J. Doctoral Dissertation, University of Duisberg, F.R.G., 1989.

Table I. Wavenumbers[a] of ν(C–O) Bands (cm^{-1}) of $M(CO)_5L$ Intermediates As Used for Monitoring Kinetics by Time-Resolved IR (*n*-Heptane Solution at 25 °C)

L	Cr	Mo	W
n-heptane	1960	1969	1958
	1938	1931	1929
H_2	1975	1978	1972
		1951	
N_2	1974	1977	1972
NBD	1956	1958	1954[c]
	1947[b]		
NBN	1956		

[a] Band positions ±2 cm^{-1}. [b] This band is present as a shoulder. [c] FTIR spectrum; see Table V.

crystals, contaminated with only 5% (η^4-NBD)W(CO)$_4$. (See Table V for IR and Table VII for ^{13}C NMR data). High-resolution mass spectrum: *m/e* [M(–CO)]$^+$ obs 424.0643, calc 424.0639 [(NBD)$_2{}^{184}$W(CO)$_2$]$^+$.

Apart from the isolation of (η^4-NBD)(η^2-NBD)W(CO)$_3$ and the preparation of (NBD)M(CO)$_4$ (M = Cr, Mo, and W) at the Max Planck Institut für Strahlenchemie, all of the experimental work described in this paper was carried out at the University of Nottingham.

Results

A. Time-Resolved IR Measurements on the Reactions of M(CO)$_6$. The primary photochemistry of Cr(CO)$_6$ in cyclohexane solution has been studied extensively by both conventional flash photolysis[11] and TRIR.[12,13] These studies show that Cr(CO)$_5$(C$_6$H$_{12}$) (i.e., Cr(CO)$_5$ with a molecule of solvent acting as a token ligand) is formed very fast, on a picosecond time scale. Cr(CO)$_5$(C$_6$H$_{12}$) then reacts more slowly (microsecond time scale) with other species (e.g., CO) in solution. Although studied in less detail, Mo(CO)$_6$ and W(CO)$_6$ behave similarly[4,14] with formation of M(CO)$_5$(solvent).

In this section, we report TRIR measurements on the reaction kinetics of M(CO)$_5$(*n*-hept) with species likely to be found in the catalytic hydrogenation mixture (e.g., CO, H_2, NBD, etc.). Table I summarizes the wavenumbers of the various species monitored by TRIR. The assignment of the bands is relatively straightforward; the frequencies of W(CO)$_5$(*n*-hept) are already known,[5] the band of Cr(CO)$_5$(*n*-hept) are very close to those of Cr(CO)$_5$(C$_6$H$_{12}$),[3,12,13] and the spectrum of Mo(CO)$_5$(*n*-hept) is similar to that of Mo(CO)$_5$ in low-temperature matrices.[15]

The kinetic data for the reactions of M(CO)$_5$(*n*-hept) [M = Cr, Mo, and W] are summarized in Table II. These data were derived from TRIR traces like those shown in Figure 1 for the reaction of Cr(CO)$_5$(*n*-hept) with NBN and NBD (see above for experimental details). The key point which emerges from data in Table II is that the rate constants for the decay of M(CO)$_5$(*n*-hept) in the presence of NBD and H_2 are strikingly similar (eqs 3 and 4). Thus, under the conditions typically found in a

$$M(CO)_5(s) + NBD \xrightarrow[M = Mo,\ k_2 = 1.7 \times 10^7\ M^{-1}\ s^{-1}]{M = Cr,\ k_2 = 1.9 \times 10^7\ M^{-1}\ s^{-1}} M(CO)_5(NBD) \quad (3)$$

$$M(CO)_5(s) + H_2 \xrightarrow[M = Mo,\ k_2 = 1.5 \times 10^7\ M^{-1}\ s^{-1}]{M = Cr,\ k_2 = 1.6 \times 10^7\ M^{-1}\ s^{-1}} M(CO)_5(H_2) \quad (4)$$

hydrogenation reaction,[16] M(CO)$_5$(*n*-hept) would be expected to react with diene rather than H_2, given the much higher concentration of diene in solution. Only in high pressure hydrogenation experiments, such as those of Mirbach and co-workers,[17] might the concentration of dissolved H_2 be sufficiently high to make formation of Cr(CO)$_5$(H_2) competitive with that of Cr(CO)$_5$(NBD).

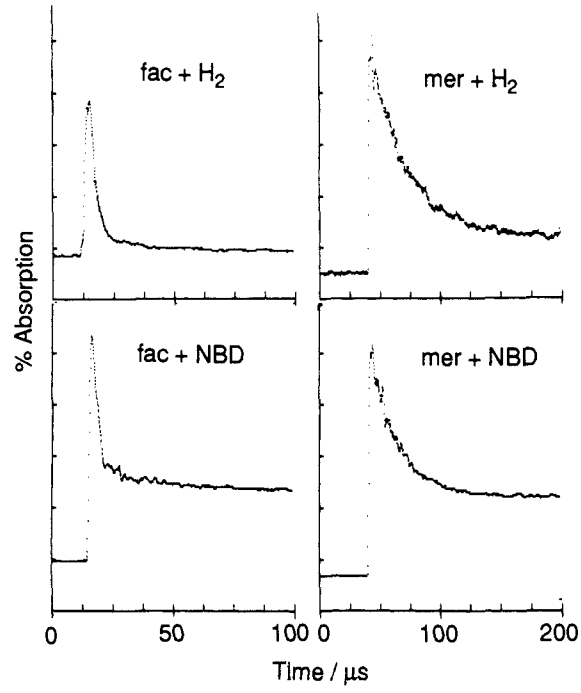

Figure 1. TRIR kinetic traces showing the reactions of Cr(CO)$_5$(s) in *n*-heptane at 25 °C: (a) decay of Cr(CO)$_5$(s) (1960 cm^{-1}) in the presence of NBD (1.0×10^{-2} M), and (c) the corresponding growth of Cr(CO)$_5$(NBD) (1956 cm^{-1}); (b) decay of Cr(CO)$_5$(s) (1960 cm^{-1}) in the presence of NBN (1.0×10^{-2} M), and (d) the corresponding growth of Cr(CO)$_5$(NBN) (1956 cm^{-1}). For rate constants, see Table II. Note that, at the resolution of our TRIR apparatus, there is some overlap between IR bands of Cr(CO)$_5$(s) and Cr(CO)$_5$(L), so that the traces (a) and (c) do not return completely to the baseline after the decay of Cr(CO)$_5$(s). Fortunately, this overlap does not prevent the kinetic analysis of the traces.

The formally "unsaturated" intermediates M(CO)$_5$(*n*-hept) appear to react somewhat faster than the corresponding M(CO)$_5$(cyclohexane) species.[12,14] Rate constants in heptane are about twice those in cyclohexane, which is consistent with *n*-heptane acting as a slightly weaker token ligand than cyclohexane. However, these differences in rate constants are small on an absolute scale, and our conclusions should be equally valid in both solvents.

The kinetic data also show that M(CO)$_5$(*n*-hept) reacts rather more slowly with the hydrogenated product, norbornene (NBN), than it reacts with NBD[18] (see Figure 1). Thus, in normal circumstances, it is only in the later stages of the reaction that reaction with NBN would become significant. However, by that time the solution is unlikely to contain much M(CO)$_6$ and hence M(CO)$_5$(solvent), because most of the metal will be in the form of olefin or diene complexes. (η^2-NBD)M(CO)$_5$ species are short-lived under the conditions of photocatalytic hydrogenation at room temperature (see below).[19] Thus, the most important kinetic measurements will be those involving (NBD)M(CO)$_4$ and their photoproducts.

(11) Kelly, J. M.; Bent, D. V.; Hermann, H.; Schulte-Frohlinde, D.; Koerner von Gustorf, E. A. *J. Organomet. Chem.* **1974**, *69*, 259. Bonneau, R.; Kelly, J. M.; Long, C. *J. Phys. Chem.* **1983**, *87*, 3344. Simon, J. D.; Xie, X. *J. Phys. Chem.* **1986**, *90*, 6751.

(12) Church, S. P.; Grevels, F.-W.; Hermann, H.; Schaffner, K. *Inorg. Chem.* **1984**, *23*, 3830; **1985**, *24*, 418.

(13) Wang, L.; Zhu, X.; Spears, K. G. *J. Am. Chem. Soc.* **1988**, *110*, 8695.

(14) Skibbe, V. Doctoral Dissertation, University of Duisberg, F.R.G., 1985.

(15) Perutz, R. N.; Turner, J. J. *Inorg. Chem.* **1975**, *14*, 262.

(16) (a) Koerner von Gustorf, E. A.; Grevels, F.-W. *Fortschr. Chem. Forsch.* **1969**, *13*, 366. (b) Platbrood, G.; Wilputte-Steinert, L. *J. Organomet. Chem.* **1974**, *70* 393; **1974**, *70*, 407. (c) Fischler, I.; Budzwait, M.; Koerner von Gustorf, E. A. *J. Organomet. Chem.* **1976**, *105*, 325.

(17) Mirbach, M. J.; Phu, T. N.; Saus, A. *J. Organomet. Chem.* **1982**, *236*, 309.

(18) For Cr(CO)$_5$(*n*-hept), the rate of reaction with NBD is (allowing for experimental error) exactly twice that with NBN (at equal concentrations of NBD and NBN). This may well be fortuitous, but it is tempting to correlate these rates with the availability of two nucleophilic sites (the C=C bonds) in NBD compared with only one in NBN.

(19) The reactions of (η^2-NBD)Mo(CO)$_5$ have been studied in some detail by Dobson and co-workers. Zhang, S.; Dobson, G. R. *Abstract of Papers*, National Meeting of the American Chemical Society, Miami, 1989; American Chemical Society: Washington, DC, 1989; INOR 266.

Table II. Kinetic Data for Decay of $M(CO)_5$(*n*-heptane) with L[a]

M	L	[L]/M	k_{obs}/s^{-1} decay	k_{obs}/s^{-1} growth of $M(CO)_5L$	k_2/m^{-1} s^{-1}
Cr	H_2	3.8×10^{-3} [b]	6.2×10^4	6.3×10^4	1.6×10^7
	N_2	1.1×10^{-2} [c]	6.9×10^4	6.6×10^4	6.2×10^6
	NBD	5.0×10^{-3}	9.0×10^4	5.1×10^4	1.8×10^7
	NBD	1.0×10^{-2}	1.9×10^5	-	1.9×10^7
	NBD	2.0×10^{-2}	4.0×10^5	-	2.0×10^7
	NBD[d]	0.1	1.3×10^6	-	1.3×10^7
	NBN	1.0×10^{-2}	8.4×10^4	8.8×10^4	8.4×10^6
	Ar	*e*	5.0×10^3		-
Mo	H_2	3.8×10^{-3}	5.8×10^4	5.7×10^4	1.5×10^7
	N_2	1.1×10^{-2}	6.6×10^4	6.6×10^4	6.0×10^6
	NBD	5.0×10^{-3}	8.6×10^4	8.6×10^4	1.7×10^7
	NBN	1.0×10^{-2}	1.2×10^5	1.1×10^5	1.2×10^7
W	H_2	3.8×10^{-3}	4.9×10^3	4.9×10^3	1.9×10^6
	N_2	1.1×10^{-2}	5.9×10^3	3.6×10^3	5.4×10^5
	CO	1.1×10^{-2} [f]	8.3×10^3	-	7.5×10^5
	Ar	-	6.7×10^2	-	

[a] All measurements made by TRIR at 25 °C; for monitoring frequencies see Table I. The concentration of dissolved carbonyl compound is 5×10^{-4} M. [b] 1 atm of $H_2 = 3.8 \times 10^{-3}$ M (see ref 2). [c] Assuming N_2 has a similar solubility to CO. [d] The value of k_2, as calculated from a plot of k_{obs} vs [NBD], is 1.9×10^7 M^{-1} s^{-1}. [e] Under 1 atm of Ar, where the reaction of $Cr(CO)_5$(*n*-heptane) is with photoejected CO or trace impurities in solution. [f] 1 atm of CO = 1.1×10^{-2} M.

Table III. Rate Constants[a] for the Decay of *fac*- and *mer*-(NBD)$M(CO)_3$(s) (s = *n*-Heptane) in the Presence of Various Ligands at 25 °C

fac-(NBD)-$M(CO)_3$(s)	L	[L]/M	k_{obs}/s^{-1}	k_2/M^{-1} s^{-1}
M = Mo[b]	Ar	-	1.1×10^5	-
	CO	1.1×10^{-2}	3.9×10^5	2.5×10^7
	N_2	1.1×10^{-2}	4.4×10^5	3.0×10^7
	H_2	3.8×10^{-3}	2.5×10^5	3.7×10^7
	NBD	5.0×10^{-3}	3.1×10^5	4.0×10^7
M = W[e,f]	Ar	-	4.6×10^4	-
	CO	1.1×10^{-2}	3.3×10^5	2.5×10^7
	H_2	3.8×10^{-3}	6.9×10^4	6.0×10^6
mer-(NBD)-$M(CO)_3$(s)	L	[L]/M	k_{obs}/s^{-1}	k_2/M^{-1} s^{-1}
M = Mo[d]	Ar	-	2.4×10^4	-
	CO	1.1×10^{-2}	6.8×10^4	4.0×10^6
	N_2	1.1×10^{-2}	3.4×10^4	9.0×10^5
	H_2	3.8×10^{-3}	3.0×10^4	1.3×10^6
	NBD	5.0×10^{-3}	4.2×10^4	3.5×10^6
M = W[e,f]	Ar	-	2.2×10^4	-
	CO	1.1×10^{-2}	2.8×10^4	4.6×10^5
	H_2	3.8×10^{-3}	2.5×10^4	7×10^5

[a] For details of calculations of k_2, see ref 6. [b-e] Monitoring wavenumbers (cm^{-1}): 1888 (*b*), 1890 (*c*), 1944 (*d*), 1884 (*e*). [f] The uncertainty in the rate constants for W are somewhat greater than those for Mo because of overlap between the IR bands of the *mer* and *fac* intermediates.

B. The Reactions of (NBD)$M(CO)_4$ with Diene and Dihydrogen. The primary photoproducts formed upon flash photolysis of (NBD)$M(CO)_4$ have already been identified as *fac*- and *mer*-(NBD)$M(CO)_3$ in our first paper.[1] Table III summarizes rate constant data for *fac*- and *mer*-(NBD)$M(CO)_3$ (M = Mo and W) in the presence of various ligands (e.g., H_2, N_2, etc.). Several points emerge from the table:

(i) For the same metal, the *fac* and *mer* intermediates react at substantially different rates. This indicates that there is no isomerization of *fac* ⇌ *mer* on the time scale of their lifetime in solution. We have previously described similar effects in the flash photolysis of $W(CO)_4LL'$ compounds, where the cis isomer of $LW(CO)_4$(s) reacted substantially faster than the trans isomer.[5]

(ii) The rate constants for *fac*-(NBD)$Mo(CO)_3$ are nearly 1 order of magnitude greater than those for the *mer* isomer. One possible rationalization of this difference in reactivity is to assume that, like other "unsaturated" intermediates, these species have a token solvent ligand occupying the vacant coordination site. Steric and electronic factors in the *fac* configuration might then labilize the token ligand.

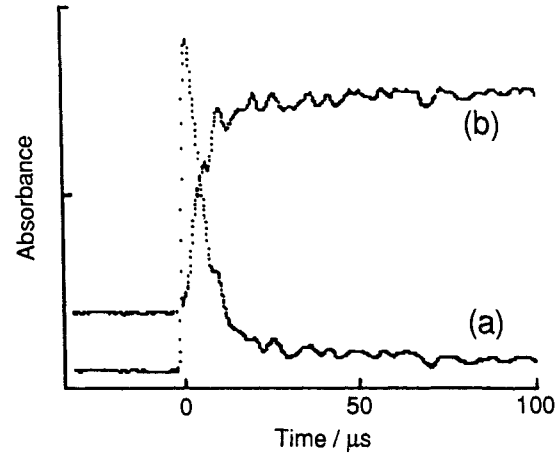

Figure 2. TRIR kinetic traces recorded during the flash photolysis of (NBD)$Mo(CO)_4$ in *n*-heptane under 1 atm of H_2. The traces show (a) the formation and decay of *fac*-(NBD)$Mo(CO_3)$(s) (monitored at 1888 cm^{-1}) and (b) the formation of *fac*-(NBD)$Mo(CO)_3(H_2)$ (monitored at 1930 cm^{-1}).

(iii) The reactions appear to be stereospecific. Thus, *fac*-(NBD)$Mo(CO)_3$ reacts to form *fac*-(NBD)$Mo(CO)_3$(L) (see Figure 2), but it is not formed from *mer*-(NBD)$Mo(CO)_3$.

(iv) The crucial observation is that for each of the two isomers, *mer*- and *fac*-(NBD)$Mo(CO)_3$(s), the rate constant for reaction with H_2 is very close[20] to that for reaction with NBD (eqs 5 and 6 and Figure 3). This behavior parallels exactly what was found

$$\textit{mer}\text{-(NBD)Mo(CO)}_3\text{(s)} + \text{L} \xrightarrow[\text{L = H}_2,\ k_2 = 1.3 \times 10^6\ \text{M}^{-1}\ \text{s}^{-1}]{\text{L = NBD},\ k_2 = 3.5 \times 10^6\ \text{M}^{-1}\ \text{s}^{-1}} \textit{mer}\text{-(NBD)Mo(CO)}_3\text{(L)} \quad (5)$$

$$\textit{fac}\text{-(NBD)Mo(CO)}_3\text{(s)} + \text{L} \xrightarrow[\text{L = H}_2,\ k_2 = 3.7 \times 10^7\ \text{M}^{-1}\ \text{s}^{-1}]{\text{L = NBD},\ k_2 = 4.0 \times 10^7\ \text{M}^{-1}\ \text{s}^{-1}} \textit{fac}\text{-(NBD)Mo(CO)}_3\text{(L)} \quad (6)$$

for $M(CO)_5$(*n*-hept) (see above), and the implications are the same. *The unsaturated intermediates in this reaction show little discrimination between incoming ligands*, presumably because loss of the token *n*-heptane ligand is the rate-determining step. Thus, in the hydrogenation mixture, the reaction of the primary photoproducts, (NBD)$Mo(CO)_3$(solvent), with H_2 is an unlikely event,

(20) At a qualitative level, the Cr intermediates appear to behave in the same way as their Mo analogues, although the rates were too fast to measure quantitatively on our TRIR apparatus.

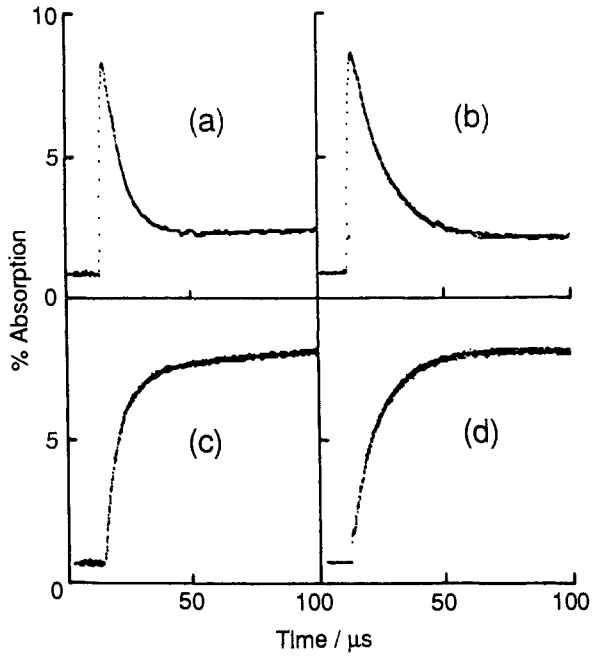

Figure 3. TRIR kinetic traces showing the differences in reaction rates of *fac*-(NBD)Mo(CO)$_3$(*n*-hept) (monitored at 1888 cm^{-1}) and *mer*-(NBD)Mo(CO)$_3$(*n*-hept) (monitored at 1944 cm^{-1}). It is clear from these traces how, for each isomer, the rates of reaction with H_2 (ca. 4 × 10^{-3} M) and NBD (5 × 10^{-3} M) are very similar (see also Table III). Note that, for the reaction with NBD, there is significant overlap between the IR absorptions of the (NBD)Mo(CO)$_3$(*n*-hept) intermediates and those of the (NBD)(η^2-NBD)Mo(CO)$_3$ products. Thus, there is residual absorption in the kinetic traces after the (NBD)Mo(CO)$_3$(*n*-hept) intermediate has reacted. However, as in Figure 1, this residual absorption does not prevent the kinetic analysis of the traces.

because the concentration of NBD is much higher than that of H_2.

This conclusion is of considerable significance. All of the mechanisms suggested for the catalytic hydrogenation have made the implicit[22] or explicit[17] assumption that unsaturated intermediates derived from (NBD)M(CO)$_4$ will react preferentially with H_2. This assumption is inconsistent with our measured rate constants, which indicate that (η^4-NBD)(η^2-NBD)M(CO)$_3$ species will be formed. Our TRIR experiments show that the lifetime of such species are quite long (>40 ms) and several related (η^4-NBD)(η^2-alkene)M(CO)$_3$ have been isolated.[10,21,23] These observations have prompted us to search for the presence of (η^4-NBD)(η^2-NBD)M(CO)$_3$ compounds in solution during catalytic hydrogenation.

C. FTIR Studies during Catalytic Hydrogenation. In this section, we use FTIR to identify long-lived carbonyl species in catalytic solutions at room temperature (the detailed procedure is described in the Experimental Section). First, we demonstrate that catalytic hydrogenation is indeed occurring under the conditions used and then we examine the metal carbonyl species present in the solution.

(a) IR Evidence for Catalytic Activity. Catalytic activity was detected through the ν(C–D) bands[24] generated by carrying out the "hydrogenation" under a pressure of D_2. Figure 4 compares the ν(C–D) bands produced in three similar deuteration experiments,[25] where a high-pressure Hg arc was used to irradiate NBD and (a) Cr(CO)$_6$, (b) Mo(CO)$_6$, or (c) W(CO)$_6$. Two points are clear from these spectra; firstly, under these photolysis conditions, W(CO)$_6$ is an extremely poor catalyst compared to the other two metals, and secondly, Cr and Mo do not give the same distribution of products.

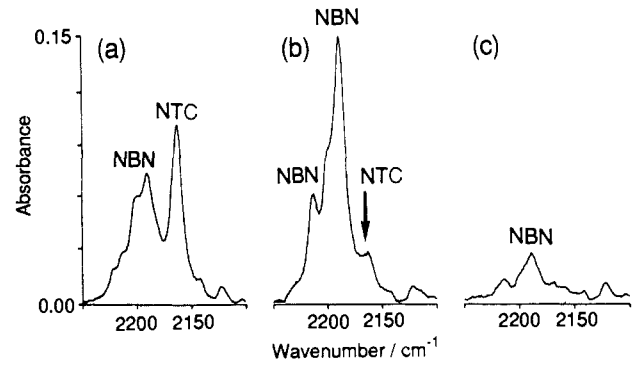

Figure 4. IR spectra in the ν(C–D) region recorded after prolonged (20 h) photolysis with a high-pressure Hg arc of (a) Cr(CO)$_6$, (b) Mo(CO)$_6$, and (c) W(CO)$_6$ with NBD and D_2 in *n*-heptane solution. The spectra illustrate the relative efficiency of the three metals as catalysts under these conditions. The labels indicate the assignment of the stronger bands to nortricyclene (NTC) or norbornene (NBN); see Table IV.

Table IV. Wavenumbers (cm^{-1}) of the ν(C–D) IR Bands Observed after the Photocatalytic Deuteration of Norbornadiene and Other Dienes

diene	product	ν(C–D)[c]
NBD	D_2-norbornene (NBN)	2188 (2188[d])
		2212 (2212[d])
NBD	D_2-nortricyclene (NTC)	2163 (2164[d])
		(2202, weak[d])
butadiene	1,4-D_2-but-2-ene[a]	2163
1,3-cyclohexadiene	3,6-D_2-cyclohexene[b]	2165
		2150
		2121

[a] Cr catalyst,[26] ν(C–D) band is very broad [b] Cr catalyst.[24,27] [c] *n*-Heptane solution, room temperature. [d] CCl_4 solution. IR spectra of samples of D_2-NBN (96%) and D_2-NTC (>99% purity) separated by preparative-scale GLC from the deuteration of NBD with a (NBD)-Cr(CO)$_4$ catalyst at the Max Planck Institut für Strahlenchemie.

The difference between Cr and the other metals was reported by Darensbourg and co-workers,[22] who showed that, with Mo(CO)$_6$ or W(CO)$_6$ as catalysts, the hydrogenation of NBD produced predominantly norbornene (NBN) whereas, with Cr(CO)$_6$, nortricyclene (NTC) is the major product. Thus, it is reasonable to assign the strongest ν(C–D) bands to NBN and NTC as shown in Figure 4. These assignments have been confirmed by recording the IR spectra of D_2-NTC and D_2-NBN, both isolated by preparative-scale GLC (Table IV).

We have also examined the hydrogenation of 1,3-cyclohexadiene and butadiene using this ν(C–D) technique. The experiments have shown that Cr(CO)$_6$ is an extremely effective catalyst in both cases[26] (eqs 7 and 8). The ν(C–D) bands for the products 3,6-

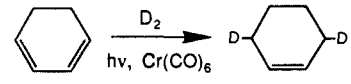

(7)

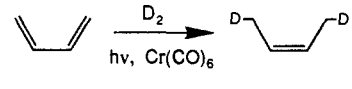

(8)

(21) Grevels, F.-W.; Skibbe, V. *J. Chem. Soc., Chem. Commun.* **1984**, 681. (b) Grevels, F.-W.; Jacke, J.; Klotzbücher, W. E.; Ozkar, S.; Skibbe, V. *Pure Appl. Chem.* **1988**, *60*, 1017.

(22) Darensbourg, D. J.; Nelson, H. H., III. *J. Am. Chem. Soc.* **1974**, *96*, 6511. Darensbourg, D. J.; Nelson, H. H., III; Murphy, M. A. *J. Am. Chem. Soc.* **1977**, *99*, 896.

(23) Grevels, F.-W.; Jacke, J.; Klotzbücher, W. E. Unpublished results.

(24) The proof that these bands are a direct result of performing the reaction with D_2 comes from carrying out the same reaction with H_2. The ν(C–D) bands were only present when D_2 is used, while the ν(C–O) regions in the two experiments are identical. In the case of NBN and NTC and cyclohexene, we separated samples of the deuterated products which had ^{1}H NMR spectra in agreement with those reported by previous workers (Werstiuk, N. H. *Can. J. Chem.* **1970**, *48*, 2310. Platbrood, G.; Wilputte-Steinert, L. *Bull. Soc. Chim. Belg.* **1973**, *82*, 733). In addition we recorded the ^{13}C NMR spectra of deuterated NBN and NTC.

(25) Although the external factors (i.e., apparatus, UV lamp, irradiation time, reagent concentrations, etc.) were the same in all three experiments, the number of quanta absorbed will necessarily be somewhat different because the UV/vis absorption spectra of the various species differ from one metal to another.

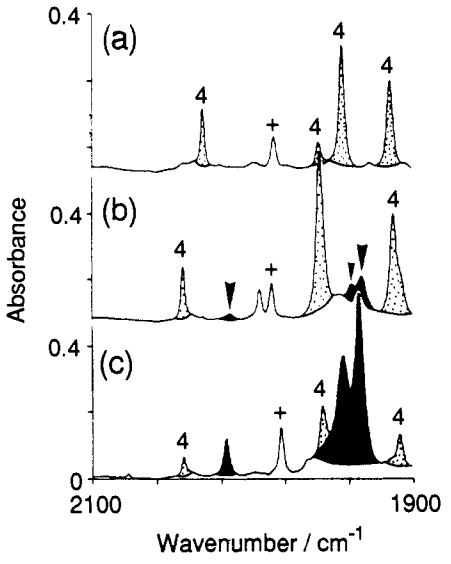

Figure 5. IR spectra in the ν(C–O) region taken after 1 h of UV photolysis of solutions in *n*-heptane containing NBD, D_2, and (a) $Cr(CO)_6$, (b) $Mo(CO)_6$, and (c) $W(CO)_6$. The spectra were recorded in the same experiments as those in Figure 4. The bands are assigned as follows: black, *mer*-(η^4-NBD)(η^2-NBD)M(CO)$_3$; 4, (η^4-NBD)M(CO)$_4$; +, residual M(CO)$_6$. (Note that, in this and subsequent figures, the shading of a band is largely to aid visualization and does not necessarily show the exact area of the particular band.)

D_2-cyclohexene and, presumably, 1,4-D_2-butene are included in Table IV. We also found that $Mo(CO)_6$ and $W(CO)_6$ did not catalyze the hydrogenation of 1,3-cyclohexadiene when irradiated with our high pressure Hg arc (>320 nm).[27]

(b) Metal Carbonyl Species in Catalytic Solution. During the hydrogenation of NBD, the IR spectrum of the solution shows substantial changes in the ν(C–O) region. For all three metals (Cr, Mo, and W), the IR spectrum changes rapidly at the start of the UV irradiation; the ν(C–O) band of $M(CO)_6$ decreases in intensity and new bands appear. As the UV irradiation proceeds, the intensities of these new bands reach a "steady state" and the spectrum remains unchanged for some considerable time. This photostationary state is established before a significant degree of hydrogenation has occurred, and, apart from a residual absorption due to $M(CO)_6$, all of the bands are assignable to complexes with one or more NBD ligands coordinated to the metal center. Thus, it is these species, or their photoproducts, that must be involved in the catalytic cycle. The wavenumbers of all ν(C–O) bands are summarized in Table V. Figure 5 illustrates the "steady state" spectra obtained, when a high pressure Hg arc was used to irradiate (a) $Cr(CO)_6$, (b) $Mo(CO)_6$, and (c) $W(CO)_6$ in the presence of NBD and D_2. All three spectra show bands due to (NBD)M(CO)$_4$, as might be expected from previous work on these systems.[16,17,22] However, the spectrum for W is strikingly different from those of the other two metals. The bands of (NBD)M(CO)$_4$, marked 4 in Figure 5, dominate the spectra of Cr and Mo but are only minor absorptions in the W spectrum (Figure 5c), where the most intense features are three bands, colored black. Similar bands are seen at lower intensity in the Mo spectrum, arrowed in Figure 5b.

Table V. Wavenumbers[a] (cm^{-1}) of the ν(C–O) IR Bands of NBD Complexes in *n*-Heptane Solution at Room Temperature

	Cr	Mo	W	assignment
(η^2-NBD)M(CO)$_5$				C_{4v}
			2078	a_1
	1956[a]	1958[a]	1954	e + a_1
(η^4-NBD)M(CO)$_4$				C_{2v}
	2031.5	2043.9	2043.7	a_1
	1958.6	(1958)	(1956)	a_1
	1944.0	1958.0	1956.5	b_1
	1914.0	1912.2	1908.8	b_2
fac-(η^4-NBD)(η^2-NBD)M(CO)$_3$				C_s
	1990[c]	*b*	1993.6	a′
	1930[c]		1926.5	a′
	1885[c]		1900.2	a″
mer-(η^4-NBD)(η^2-NBD)M(CO)$_3$				C_s
	b	2014.5	2017.5	a′
		1938.1	1943.7	a′
		1932.0	1933.4	a″
mer-(η^4-NBD)(η^2-NBN)M(CO)$_3$[d]				C_s
			2014.5	a′
			1938	a″
			1931	a′
cis-(η^2-NBD)$_2$M(CO)$_4$[f]				
			1962	
			1915.5	
cis-(η^4-NBD)$_2$M(CO)$_2$[g]				C_s
		1930[h]	1980[i]	a′
		1880[h]	1920[i]	a″

[a] Assignment for C_{4v}; e TRIR data ±2 cm^{-1}. Other wavenumbers ±0.5 cm^{-1}. [b] Not observed. [c] *fac*-(η^4-NBD)(η^2-NBD)Cr(CO)$_3$ data for LXe solution −91 °C. [d] *n*-Hexane solution; from ref 10. [f] Tentative identification, cf. *cis*-(C_2H_4)$_2$M(CO)$_4$ 1957 and 1910 cm^{-1}; ref 32. [g] Data from ref 37. [h] Solid state, KBr disk. [i] $CDCl_3$ solution.

These three bands can be assigned to the ν(C–O) vibrations (2a′ + a″) of *mer*-(η^4-NBD)(η^2-NBD)M(CO)$_3$ (M = Mo and W) for the following reasons. Identical bands are observed when $M(CO)_6$ and NBD are irradiated in the presence of H_2, D_2, or Ar,[28] but the bands are not observed in the absence of NBD. The same bands appear in the spectrum after the photolysis of (NBD)M(CO)$_4$ in the presence of NBD. For both metals, the three bands are similar in both wavenumber and relative intensity to the spectra of several well-characterized *mer*-(η^4-NBD)(η^2-alkene)M(CO)$_3$ compounds.[21,23] These conclusions are strengthened further by ^{13}C NMR data (see below).

In the absence of air, a solution of *mer*-(η^4-NBD)(η^2-NBD)-W(CO)$_3$ is stable indefinitely, and the compound only decays slowly (over a period of ca. 2 h) after exposure of the solution to air. *mer*-(η^4-NBD)(η^2-NBD)Mo(CO)$_3$ is somewhat more air-sensitive and decomposes completely within an hour. It is clear from the spectra in Figure 5 that a chromium complex, (η^4-NBD)(η^2-NBD)Cr(CO)$_3$, was not detectable under these conditions. Either the (η^4-NBD)(η^2-NBD)Cr(CO)$_3$ complexes are not formed at all or else they are thermally too unstable to be detected. Thermal instability seems to be the more probable explanation, particularly because we have evidence[29] for the formation of *fac*-(η^4-NBD)(η^2-NBD)Cr(CO)$_3$ in LXe solution at −90 °C (see Table V).

(c) The Role of *mer*-(η^4-NBD)(η^2-NBD)M(CO)$_3$ in Catalysis. The spectra in Figures 4 and 5 suggest that there may be a negative correlation between catalytic activity and the presence of *mer*-(η^4-NBD)(η^2-NBD)M(CO)$_3$. Apparently, more deuteration occurs when there is no *mer*-(η^4-NBD)(η^2-NBD)M(CO)$_3$ in solution. This hypothesis is dramatically confirmed by irradiating the tungsten system with different UV lamps, an experiment which underlines the great wavelength sensitivity[1] of the system. When a $W(CO)_6$/NBD/D_2 mixture is irradiated with

(26) It is surprising that, although the catalytic hydrogenation of isoprene has been well studied,[16] there do not appear to be any reports of hydrogenating butadiene by this route before.

(27) Fortuitously, the inability of Mo to catalyze the hydrogenation of 1,3-cyclohexadiene (CHD) under these conditions provided a good indication of the sensitivity of our ν(C–D) method for detecting catalytic activity. One of our experiments involved an attempt to use (NBD)Mo(CO)$_4$ as a hydrogenation catalyst for CHD, with a ratio (NBD)Mo(CO)$_4$/CHD of 1:100. After several hours photolysis with a high pressure Hg arc, there was no evidence for the ν(C–D) bands of 3,6-dideuterocyclohexene but the ν(C–D) band of deuterated NBN was easily observed. This suggests a detection limit of $<10^{-4}$ M with a 1-mm-pathlength IR cell. CHD can, however, be photohydrogenated by (NBD)Mo(CO)$_4$, when irradiated with a medium-pressure Hg arc (Pyrex filtered).

(28) There were slight differences between the spectra produced by the reaction of NBD with $W(CO)_6$ under catalytic conditions (i.e., a pressure of D_2) and those produced under conditions where hydrogenation does not take place (i.e., under a pressure of argon). In the latter case, the bands tentatively assigned to *cis*-(η^2-NBD)$_2$W(CO)$_4$ were somewhat more intense than in the presence of D_2.

(29) Jackson, S. A. Ph.D. Thesis, University of Nottingham, UK, 1988.

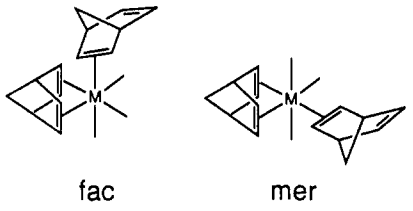

a filtered medium pressure Hg arc (>320 nm), *mer*-(η^4-NBD)(η^2-NBD)W(CO)$_3$ is the predominant carbonyl species in solution and little deuteration is observed, even after 20 h of irradiation (Figure 6a). If the same solution (in the same container) is then irradiated for only 1 h more with a tungsten filament UV sunlamp,[30] the ν(C–O) bands of *mer*-(η^4-NBD)(η^2-NBD)W(CO)$_3$ disappear completely, and significant deuteration occurs as shown by the ν(C–D) bands of norbornene (Figure 6b). The ν(C–O) spectrum is now dominated by the bands of (NBD)W(CO)$_4$ and three other bands, labeled "F", which are similar in frequency and intensity to those of *fac*-(η^4-NBD)(η^2-trcyo)W(CO)$_3$ (trcyo = *trans*-cyclooctene).[10,23] It is therefore reasonable to assign these bands to the previously unknown isomer *fac*-(η^4-NBD)(η^2-NBD)W(CO)$_3$. However, unlike the trcyo compound, *fac*-(η^4-NBD)(η^2-NBD)W(CO)$_3$ does not decay thermally into the *mer* isomer on the time scale of the experiment (ca. 1 h).[31] Figure 7 compares the ν(C–O) bands of *mer*- and *fac*-(η^4-NBD)(η^2-NBD)W(CO)$_3$ (obtained by computer subtraction). There are two further, rather weaker, ν(C–O) bands, arrowed in Figure 6, that are so far unassigned. These bands are not due to the NBD complexes, (η^2-NBD)W(CO)$_5$, *cis*-(η^4-NBD)$_2$W(CO)$_2$, or *mer*-(η^4-NBD)(η^2-NBN)W(CO)$_3$, the IR absorptions of which are all known (see Table V). In the absence of other data, we suggest that these bands may be due to *cis*-(η^2-NBD)$_2$W(CO)$_4$ by comparison with bands of other (η^2-alkene)$_2$W(CO)$_4$ species.[21,32] However the definitive identification of this species is probably not important because it is unlikely to be a key compound in the catalytic cycle. Its ν(C–O) bands have similar intensities in both parts of Figure 6, showing that it remains a constant but minor component of the mixture, while the catalytic activity varies substantially.

These FTIR experiments show that formation of *mer*-(η^4-NBD)(η^2-NBD)W(CO)$_3$ effectively terminates the catalytic deuteration. The compound appears to act as a "reservoir" for the catalytically active species. It is only when the photolysis lamp has the appropriate output (i.e. <320 nm) to tap this reservoir that significant catalysis occurs. The spectra in Figure 6 indicate that, under these conditions, photolysis of *mer*-(η^4-NBD)(η^2-NBD)W(CO)$_3$ has the overall effect of either loss of the η^2-NBD group (ultimately to form (NBD)W(CO)$_4$) or isomerization to *fac*-(η^4-NBD)(η^2-NBD)W(CO)$_3$. This is consistent with our previous observation[1] that photolysis of *mer*-(η^4-NBD)(C$_2$H$_4$)Mo(CO)$_3$ in LXe leads to loss of C$_2$H$_4$ and formation of *fac*-(η^4-NBD)Mo(CO)$_3$L species.

The IR spectra in Figure 6b clearly show that the catalytic solution also contains *fac*-(η^4-NBD)(η^2-NBD)W(CO)$_3$.[31] It is therefore important to know how such species behave under photolytic conditions before proposing an overall scheme for the deuteration of NBD. Unfortunately *fac*-(η^4-NBD)(η^2-NBD)W(CO)$_3$ has not yet been isolated, and the only model complexes available at room temperature are *fac*-(η^4-NBD)(η^2-trcyo)M(CO)$_3$ (M = Mo and W), which involve a rather atypical alkene. We therefore decided to generate *fac*-(η^4-NBD)(C$_2$H$_4$)M(CO)$_3$ compounds in LXe solution to use as models.

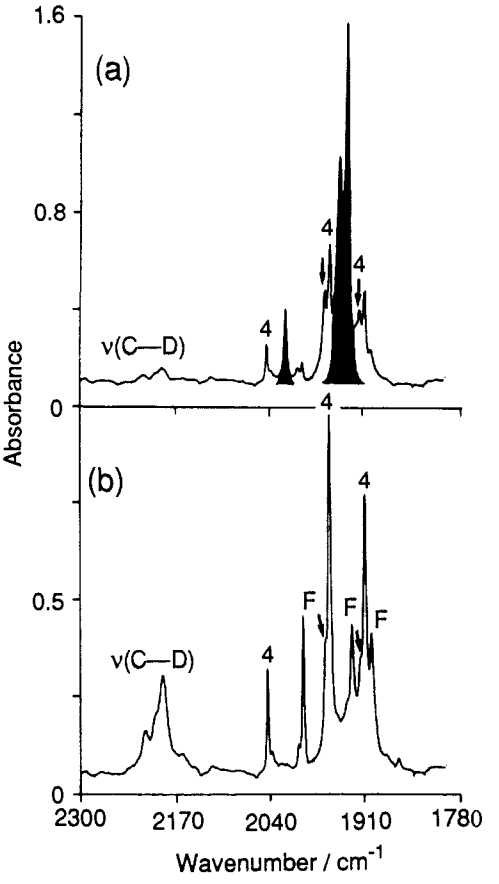

Figure 6. IR spectra in the ν(C–D) and ν(C–O) regions illustrating the wavelength dependence of the catalytic deuteration of NBD in the presence of W(CO)$_6$: (a) spectrum recorded after 20.5 h of irradiation of a solution of W(CO)$_6$, NBD and D$_2$ with a medium-pressure Hg arc, filtered >320 nm; (b) spectrum recorded after 1 h more irradiation of the same solution with a 300 W UV sunlamp. Note the substantial increase in the intensity of the bands, due largely to NBN, in the ν(C–D) region. The other bands are labeled as follows: black, *mer*-(η^4-NBD)(η^2-NBD)W(CO)$_3$; F, *fac*-(η^4-NBD)(η^2-NBD)W(CO)$_3$; 4, (η^4-NBD)W(CO)$_4$; arrowed, *cis*-(η^2-NBD)$_2$W(CO)$_4$ (tentative assignment).

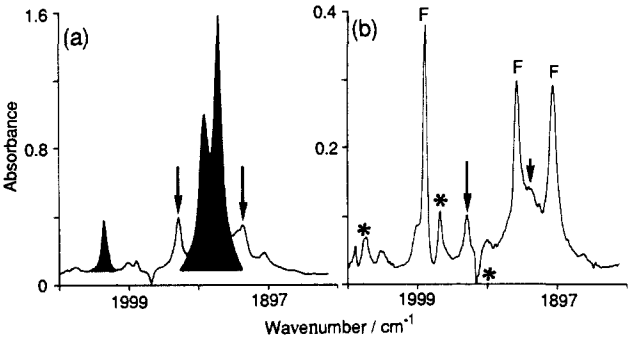

Figure 7. ν(C–O) bands of (a) *mer*, colored black, and (b) *fac*-(η^4-NBD)(η^2-NBD)W(CO)$_3$, marked F, in *n*-heptane solution. These spectra were obtained by computer subtraction of spectra similar to those in Figure 6. The arrowed bands are assigned to *cis*-(η^2-NBD)$_2$W(CO)$_4$ (see text), and the asterisks indicate artifacts produced by the computer subtraction.

(d) The Generation and Reactions of *fac*-(NBD)(C$_2$H$_4$)M(CO)$_3$ in Liquid Xenon. We have already reported[32] how thermally labile

(30) For details of photolysis, see the Experimental Section. The difference between the sunlamp (W filament) and the filtered Hg arc is due to differences in wavelength rather than intensity. The catalytic activity is almost certainly due to light in the 280–320-nm region because removal of the soda glass filter (>320 nm) from the Hg arc also produces a significant increase in photocatalytic activity which is, nevertheless, rather less dramatic than the effects of the sunlamp.

(31) This difference in thermal stability between *fac*-(η^4-NBD)(trcyo)W(CO)$_3$ and the compound which we have assigned as "*fac*-(η^4-NBD)(η^2-NBD)W(CO)$_3$" is so surprising that we tried, unsuccessfully, to find an alternative assignment for these bands. Nevertheless, it is important to stress that it is the definitive identification of *mer*-(η^4-NBD)(η^2-NBD)W(CO)$_3$ that is crucial to our mechanistic arguments. Thus, although some of our detailed discussion would clearly be altered if our identification of *fac*-(η^4-NBD)(η^2-NBD)W(CO)$_3$ were incorrect, our overall conclusions about the mechanistic role of the diene would be unaffected.

(32) Gregory, M. F.; Jackson, S. A.; Poliakoff, M.; Turner, J. J. *J. Chem. Soc., Chem. Commun.* **1986**, 1175.

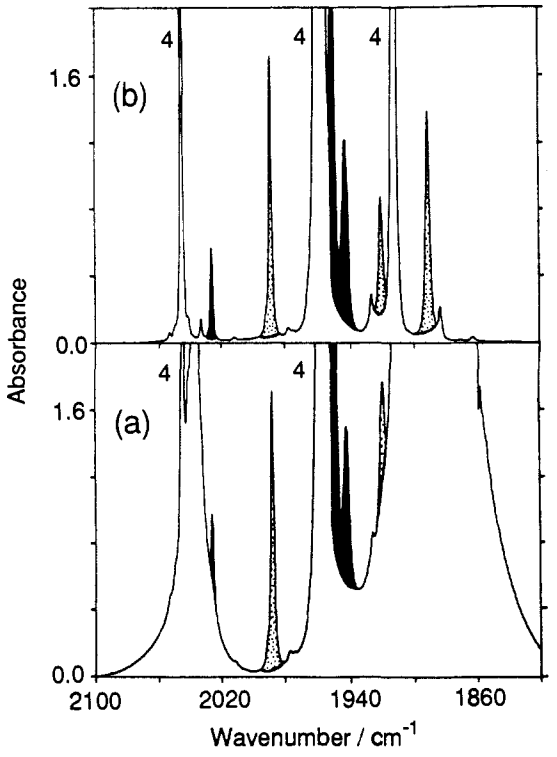

Figure 8. IR spectra in the ν(C–O) region showing the spectroscopic effect of pumping off an ethene/xenon mixture and replacing it with clean xenon: (a) spectrum showing after 10 min of UV photolysis of $(NBD)Mo(CO)_4$ in LXe doped with C_2H_4 at −90 °C; (b) spectrum showing after venting the solvent and adding pure Xe. The bands are assigned as follows: black, *mer*-$(NBD)(C_2H_4)Mo(CO)_3$; dotted, *fac*-$(NBD)(C_2H_4)Mo(CO)_3$; 4, $(\eta^4\text{-NBD})Mo(CO)_4$.

Table VI. IR Frequencies ν(C–O) (cm^{-1}) of the *mer* and *fac* Isomers of $(\eta^4\text{-NBD})(C_2H_4)M(CO)_3$ in LXe Compared to Analogous Complexes Observed by Means of Other Spectroscopic Techniques

M = L =	W[a] trcyo	W[b] C_2H_4	Mo[c] C_2H_4	Cr[c] C_2H_4	Cr[c,e] N_2	
		fac-$(\eta^4\text{-NBD})M(CO)_3L$				
	1984.3	1992	1988.1	1977.3	1987.3	a′
	1921.8	1929	1920.1	*d*	1921.9	a″
	1884.9	1887	1891.2	1885.3	1900.6	a′
		mer-$(\eta^4\text{-NBD})M(CO)_3L$				
	2020.9	2031	2026.1	2005.5	2002.7	a′
	1944.3	1940	1954	1932.6	1937.2	a″
	1940 sh		1943.3			a′

[a] From ref 10; room-temperature solution. [b] From ref 23; ethene-doped Ar matrix, 12 K. [c] LXe, −91 °C. [d] Obscured. [e] From ref 1.

C_2H_4 complexes can be generated photochemically in LXe doped with C_2H_4. In the present case, however, we have refined the technique (see the Experimental Section). The experiment involved photolysis of $(NBD)M(CO)_4$ in the presence of a large excess of C_2H_4, followed by complete evacuation of the volatiles (i.e., Xe, C_2H_4, and CO) from the cell and refilling with clean Xe. This approach has two advantages: (i) we can study the subsequent reactions of the C_2H_4 complexes in the absence of excess C_2H_4, and (ii) the removal of excess C_2H_4 unmasks regions of the IR spectrum that would otherwise be obscured.

This IR effect is particularly striking. Figure 8a shows the ν(C–O) region of the spectrum obtained after UV photolysis of $(NBD)Mo(CO)_4$ in LXe heavily doped with C_2H_4. Figure 8b shows the spectrum of the same sample after the cell has been refilled with clean Xe. The IR bands of the photoproducts are much easier to identify after the C_2H_4 has been vented. These bands are assigned to the known compound[1,21,23] *mer*-$(\eta^4\text{-NBD})(C_2H_4)Mo(CO)_3$ and to the *fac* isomer, previously observed in matrix isolation experiments[23] (for IR frequencies see Table VI). Both isomers are stable in clean LXe solution at −90 °C.

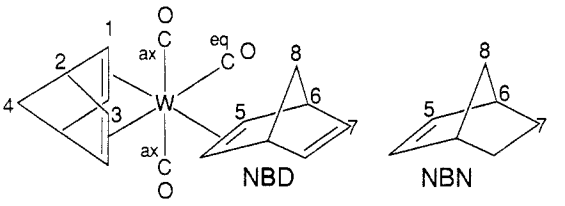

Figure 9. Numbering scheme of atoms for the ^{13}C NMR spectra of *mer*-$(\eta^4\text{-NBD})(\eta^2\text{-NBD})W(CO)_3$ and *mer*-$(\eta^4\text{-NBD})(\eta^2\text{-NBN})W(CO)_3$.

Subsequent UV photolysis of these C_2H_4 complexes[33] in the presence of added N_2 led to loss of C_2H_4 and formation of the same dinitrogen complexes as observed from the photolysis pure $(NBD)Mo(CO)_4$. There was, however, one important difference. In contrast to the photolysis of $(NBD)Mo(CO)_4$ itself,[1] significant quantities of *mer*-$(NBD)Mo(CO)_3(N_2)$ were formed even on brief UV photolysis. We shall see that this has important implications for the overall mechanism of the catalytic cycle. Thus, the predominant photochemical process in *fac*-$(\eta^4\text{-NBD})(C_2H_4)Mo(CO)_3$ appears to be loss of C_2H_4. It seems reasonable, therefore, to suppose that the behavior of *fac*-$(\eta^4\text{-NBD})(\eta^2\text{-NBD})M(CO)_3$ complexes would be similar (eq 9).

$$fac\text{-}(\eta^4\text{-NBD})(\eta^2\text{-NBD})M(CO)_3 \xrightarrow{h\nu} (\eta^4\text{-NBD})M(CO)_3(s) + NBD \quad (9)$$

Experiments with $(NBD)Cr(CO)_4$ led to the formation of the analogous Cr compounds. *fac*-$(\eta^4\text{-NBD})(C_2H_4)Cr(CO)_3$ is thermally unstable, reacting with trace N_2 in the LXe solution to form *fac*-$(\eta^4\text{-NBD})Cr(CO)_3(N_2)$. Typically, this decay was complete in about 16 h at −90 °C during which time *mer*-$(\eta^4\text{-NBD})(C_2H_4)Cr(CO)_3$ was stable. Raising the temperature of the solution to −71 °C caused the *mer* isomer to decay with a half-life of about 30 min.[34] At this temperature, the *fac* isomer could only be detected if an IR spectrum were recorded during UV irradiation.

For both Cr and Mo, our LXe experiments showed that *fac*-$(\eta^4\text{-NBD})(C_2H_4)M(CO)_3$ was formed before the *mer* isomer. This indicates that the formation of the two isomers is sequential; photolysis of the *fac* isomer leads to the *mer*. Similar observations were reported in our first paper[1] for the formation of the *fac* and *mer* isomers of $(\eta^4\text{-NBD})M(CO)_3(X_2)$ (X = H or N). The effect also has been observed previously for the formation of *mer*-$(\eta^4\text{-NBD})(\eta^2\text{-trcyo})W(CO)_3$, where the isomerization *fac* → *mer* may well be intramolecular.[21]

Our photolysis experiments at room temperature have shown that changing wavelength of the UV irradiation changes the relative amounts of *fac*- and *mer*-$(\eta^4\text{-NBD})(\eta^2\text{-NBD})W(CO)_3$ in solution. Presumably, the photoisomerization process will be similar to that in the C_2H_4 and trcyo complexes. As pointed out in our first paper,[1] there is a clear difference between our room

(33) Although the solution also contained a substantial quantity of unreacted $(NBD)Mo(CO)_4$, the amount of C_2H_4 complexes in solution were quite sufficient for us to observe any new C_2H_4/N_2 complexes if they were formed.

(34) This observation is somewhat surprising because *mer*-$(\eta^4\text{-NBD})(C_2H_4)Cr(CO)_3$ has been isolated as a stable solid at room temperature.[23] A similar observation was made with *trans*-$(C_2H_4)_2Cr(CO)_4$ which was thermally unstable when generated photochemically[32] in LXe but stable as an isolated compound.[35] The probable explanation is that, in both cases, some minor species in solution catalyses the decomposition. This is borne out by the interesting discovery[10] that silica must be added during workup after some preparative-scale photochemical reactions to sequester unidentified species which causes decomposition of the olefin complexes. Thus, it could be argued that the LXe experiments are an excellent model for the catalytic hydrogenation mixture, where decomposition might be expected since no silica is added to the mixture.

(35) Grevels, F.-W.; Jacke, J.; Ozkar, S. *J. Am. Chem. Soc.* **1987**, *109*, 7536.

(36) (a) Hooker, R. H.; Rest, A. J. *XIth Int. Conf. Organomet. Chem.*, Abstr. 36. Hooker, R. H. Ph.D. Thesis, University of Southampton, U.K., 1987. (b) Grevels, F.-W.; Jacke, J.; Klotzbücher, W. E.; Schaffner, K. *J. Organomet. Chem.*, submitted for publication, 1989.

Table VII. ^{13}C NMR Shifts (ppm) for *mer*-(η^4-NBD)(η^2-NBD)W(CO)$_3$ and *mer*-(η^4-NBD)(η^2-NBN)W(CO)$_3$

atom[a]	η^2-NBD[b,c]	η^2-NBN[b,d]
C1	79.08	78.65
C2	49.29	49.62
C3	44.74	44.28
C4	64.86	65.16
C5	65.56 br[e]	61.76
C6	47.78	41.57
C7	143.78	30.66
C8	50.06	34.35
CO-ax	204.80 br[e]	205.07
CO-eq	212.32	213.29

[a] For numbering of C atoms, see Figure 9. [b] Spectra recorded in d^8-toluene at 243 K at 100.6 MHz. [c] There is a second set of signals in the spectrum, ca. 10–20% of the intensity of the main lines, indicating that a second isomer (endo or exo) is also present. [d] For preparative details and full ^1H NMR, see ref 10. [e] Peaks broadened because rotation of η^2-NBD is not frozen out at this temperature.

temperature TRIR experiments, which show that *mer*-(η^4-NBD)M(CO)$_3$L compounds can be produced from (NBD)M(CO)$_4$ by a single-photon process and our LXe experiments, which suggest that these compounds are secondary photoproducts. This difference, which may well be due to the lower temperature in the LXe experiments, is probably not very significant for the overall catalytic cycle because even at room temperature direct formation of *mer* products is a minor process.

D. Isolation of (η^4-NBD)(η^2-NBD)W(CO)$_3$. Under the conditions of our FTIR experiments, both *fac*- and *mer*-(η^4-NBD)(η^2-NBD)W(CO)$_3$ are thermally stable at room temperature. We have succeeded in isolating a sample of the *mer* isomer (90% purity) as a brownish solid from the photochemical reaction of (NBD)W(CO)$_4$ with NBD on a preparative scale. IR spectra show that the principal contaminant is (NBD)W(CO)$_4$. The ^{13}C NMR spectrum confirms that the molecule does indeed contain two distinct NBD groups, one η^4- and the other η^2-coordinated. In addition, the spectrum is consistent with ^{13}C data for other *mer*-(η^4-NBD)(η^2-alkene)M(CO)$_3$ species[21,23] (see Table VII and Figure 9). Although no ^1H data are available, we assume that the complexes exist as a mixture of exo and endo configurations. Although a considerable number of bis-diene complexes of the group 6 metals have been characterized,[37] this compound is the first example of an η^4, η^2 bis-diene complex. In the future, our synthetic route could easily be adapted to generate compounds with two different dienes. This offers interesting possibilities for isomerization studies (eq 10).

$$(NBD)W(CO)_4 + \text{diene} \xrightarrow{h\nu} (\eta^4\text{-NBD})(\eta^2\text{-diene})W(CO)_3 \overset{\Delta}{\rightleftharpoons} (\eta^2\text{-NBD})(\eta^4\text{-diene})W(CO)_3 \quad (10)$$

Discussion

Three points of particular relevance to the hydrogenation of NBD emerge from the experiments described in this paper.

(i) The formally unsaturated species, *fac*- and *mer*-(NBD)M(CO)$_3$(*n*-hept) do not interconvert during the short time that they exist in solution.[38] Their reactions are stereospecific; *fac* intermediates lead to *fac* products, and *mer* intermediates lead to *mer* products (eqs 5 and 6).

(ii) Photolysis of (NBD)M(CO)$_4$ in the presence of NBD leads to the formation of (η^4-NBD)(η^2-NBD)M(CO)$_3$ complexes which, for Mo and W at least, are thermally stable on relatively long time scales.

Scheme I[a]

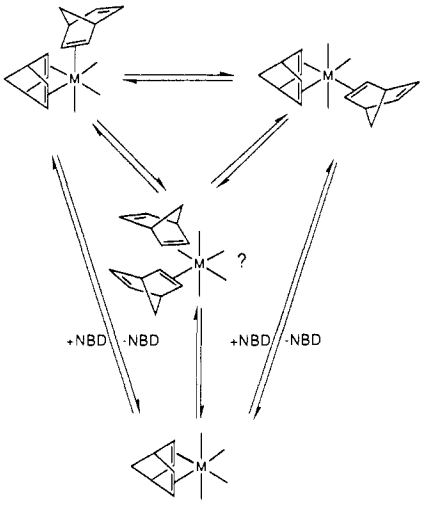

[a] M = W.

(iii) In the case of W, the catalytic mixture contains no less than four NBD complexes, which are all stable in *n*-heptane at room temperature[31,39] and which can be interconverted photochemically (Scheme I).

The behavior of *fac*- and *mer*-(NBD)M(CO)$_3$(*n*-hept) is important because in the hydrogenation step proposed in our first paper[1] these intermediates lead specifically to NTC and NBN via the *fac* and *mer* dihydrogen complexes[40] (eqs 11 and 12).

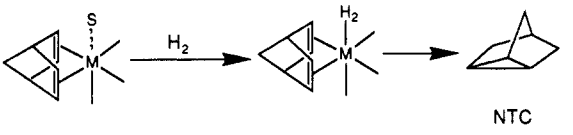

(11)

NTC

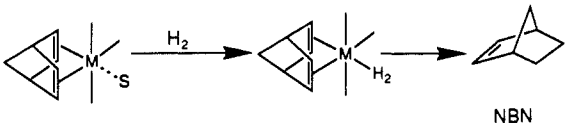

(12)

NBN

With Mo and W catalysts,[41] the principal hydrogenation product is NBN (see above) formed via *mer*-(NBD)M(CO)$_3$(H$_2$). However, our experiments[1] suggest that relatively little *mer*-(NBD)Mo(CO)$_3$(H$_2$) is formed directly from (NBD)Mo(CO)$_4$. In LXe, *mer*-(NBD)Mo(CO)$_3$(H$_2$) is mostly generated by secondary photolysis of *fac*-(NBD)M(CO)$_3$(H$_2$) (eq 13). Such a

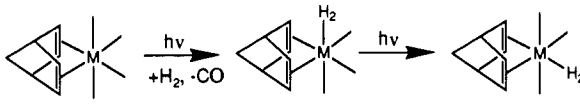

(13)

process is unlikely to occur in solution at room temperature because the lifetime of *fac*-(NBD)M(CO)$_3$(H$_2$) is too short[1] for secondary photolysis to be significant. By contrast, our experiments in LXe

(37) Kreiter, C. G. *Adv. Organomet. Chem.* **1982**, *229*, 29. Chow, T. J.; Chao, Y.-S.; Liu, L. K. *J. Am. Chem. Soc.* **1987**, *109*, 797.

(38) The photochemical *fac* ⇌ *mer* isomerization of (NBD)M(CO)$_3$ (M = Cr and Mo) has been observed in matrices,[36] but these intermediates are too short-lived in solution at room temperature for such a process to occur with the intensity of light normally used for photocatalytic hydrogenation.

(39) We have found no evidence for the formation of *trans*-(η^2-NBD)$_2$W(CO)$_4$. This compound would be expected to have only two ν(CO) IR bands (one of which would be rather weak (cf. *trans*-(C$_2$H$_4$)$_2$W(CO)$_4$ in our first paper[1])). Thus, it is possible that *trans*-(η^2-NBD)$_2$W(CO)$_4$ is formed but that its IR bands are obscured by those of other species in solution.

(40) In our first paper,[1] we showed that there might also be a route to NBN via (η^2-NBD)Mo(CO)$_4$(H$_2$). The experiments at room temperature, described above, where we observed bands tentatively assigned to (η^2-NBD)$_2$W(CO)$_4$, suggest that this pathway is relatively unimportant at least for W catalysts.

(41) For Mo and W, different ratios of NBN/NTC were observed depending on whether M(CO)$_6$ or (NBD)M(CO)$_4$ was used as the catalyst.[22] This may merely be an effect caused by different amount of free CO in solution. Photolysis of M(CO)$_6$ will lead to higher concentrations of CO in solution than are found with (NBD)M(CO)$_4$.

Scheme II

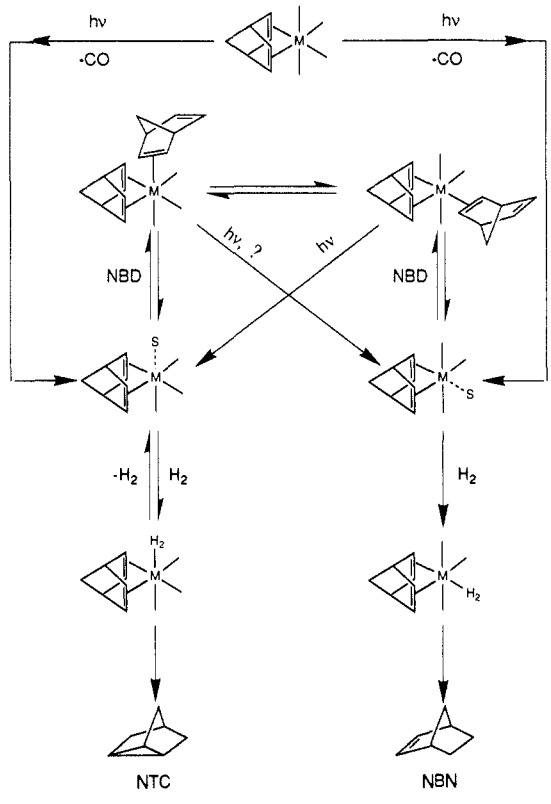

show that *mer*-(NBD)Mo(CO)$_3$(H$_2$) is formed *directly* in the photolysis of *mer*-(NBD)(C$_2$H$_4$)M(CO)$_3$ (eq 14).

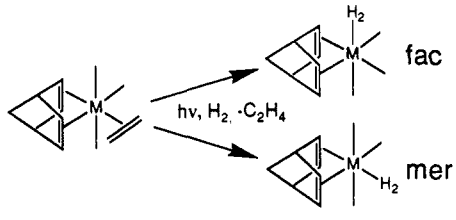

(14)

We have shown above that the *fac* and *mer* isomers of (η^4-NBD)(η^2-NBD)W(CO)$_3$ are present in catalytic mixtures at room temperature. These isomers can be interconverted photochemically. Our experiments also indicate that both isomers can lose the η^2-NBD ligand photochemically (for Cr, the process can probably also occur thermally at room temperature[42]). We therefore suggest that, in the catalytic solution at room temperature, *mer*-(NBD)M(CO)$_3$(*n*-hept) (and hence *mer*-(NBD)M(CO)$_3$(H$_2$) and, eventually, NBN; see eq 12) is generated via photolysis of these (η^4-NBD)(η^2-NBD)M(CO)$_3$ complexes.

Thus, to summarize, the proposed role of these (η^4-NBD)(η^2-NBD)M(CO)$_3$ species is 2-fold;[43] firstly, to act as a reservoir of (NBD)M(CO)$_3$(*n*-hept) intermediates and, secondly, to generate more of the *mer*-(NBD)M(CO)$_3$(*n*-hept) than would be obtained from photolysis of (NBD)M(CO)$_4$ itself. We can now combine all of the results from both of our papers to propose an overall mechanism for the hydrogenation (deuteration) of NBD (Scheme II).

The one part of the cycle omitted from Scheme II is the regeneration of the (NBD)M(CO)$_3$ moiety after hydrogenation has occurred. Although we have not studied this process in detail, a possible pathway is shown in Scheme III. The doubly unsaturated intermediate (NBN)M(CO)$_3$ is uncharacterized even

Scheme III

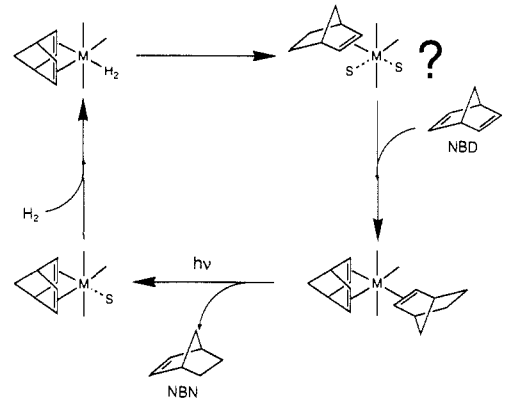

in matrices but could possibly be stabilized by agostic interactions. By contrast, *mer*-(η^4-NBD)(NBN)W(CO)$_3$ has been isolated in Mülheim[23] and is very similar in properties to the other *mer*-(η^4-NBD)(alkene)M(CO)$_3$ species discussed above (see Table V).

Conclusions

The experiments described in our two papers have shown how several spectroscopic techniques (TRIR, FTIR, LXe, etc.) can be focused onto a single mechanistic problem. When these techniques are combined with synthetic chemistry, significant new insights can be obtained even into previously well-studied reactions. Scheme II summarizes our proposed mechanism for the hydrogenation (deuteration) of NBD. It differs from earlier proposals[16,17,22] in three important ways.

(i) All of the species shown in the scheme have been identified positively by IR spectroscopy for at least two of the three group 6 metals; the rates of several of the reactions have been measured, and one compound has even been isolated from the catalytic mixture.

(ii) Nonclassical dihydrogen complexes are proposed as the key intermediates with intramolecular transfer of H$_2$ of the diene. A similar step has recently been suggested[44] for an alkene hydrogenation reaction, and such processes may well be quite widespread.

(iii) The formation of (η^4-diene)(η^2-diene)M(CO)$_3$ complexes is included as an integral part of the scheme.

In addition, our experiments have introduced two new experimental approaches: (a) the use of ν(C–D) bands for the noninvasive detection of catalytic deuteration in hydrocarbon solvents, and (b) the "pump-off" technique for generating C$_2$H$_4$ complexes in liquid Xe solution. Both techniques clearly have wider applications than the reactions studied here. We have also observed and isolated the first of a new class of (η^4-NBD)(η^2-diene)M(CO)$_3$ complexes by a route which can be applied to other compounds of this type.

We have also confirmed what appears to be quite a general observation that coordinatively unsaturated intermediates do not normally discriminate significantly between incoming ligands. Any mechanism, in which such discrimination is required, deserves close scrutiny to determine whether other pathways are possible. Equally, our experiments have underlined the unexpected role of the diene substrate in this photocatalytic hydrogenation. We suspect that there must be other catalytic systems where the reaction between intermediate and substrate has been overlooked. Such reactions should lead to the discovery of new classes of compounds just as they have done here.

Acknowledgment. We are grateful for support from EEC (Stimulation Contracts No. SC1*0007 and ST2*/00081), SERC, NATO (Grant No. 741/85), the Paul Instrument Fund, the Petroleum Research Fund, administered by the American Chemical Society, Nicolet Instruments Ltd., and Applied Pho-

(42) The possibility that this process occurs thermally for Cr is supported by our observation[10] that *mer*-(η^4-NBD)(η^2-C$_2$H$_4$)Cr(CO)$_3$ can act as a *thermal* catalyst for the hydrogenation of NBD at room temperature *in the dark*.

(43) Mirbach[17] hinted at the formation of (η^4-NBD)(η^2-NBD)Cr(CO)$_3$ as a possible step in his proposed catalytic cycle, but no information was available at that time to suggest a specific role for this species.

(44) Hampton, C.; Cullen, W. R.; James, B. R. *J. Am. Chem. Soc.* **1988**, *110*, 6618.

tophysics Ltd. M.P. thanks the Nuffield Foundation for a Research Fellowship. We thank J. M. Whalley for his technical assistance and the many people who have discussed these results with us, particularly Professors J. K. Burdett and J. A. Connor and Drs. M. A. Healy, B. P. Straughan, and R. Whyman. We are grateful to D. Chmielewski for isolating control samples of deuterated NBN and NTC. Finally, we thank the Nottingham undergraduates who have contributed to this topic through their project work: A. P. Breen, D. N. Gregory, R. M. Ingram, M. Jobling, P. A. Johnson, and M. S. Jones.

Communications to the Editor

Size of Alkyl Group R: Principal Factor Determining Wettability of Surface-Functionalized Polyethylenes (PE-CONHR and PE-CO_2R) by Water[1]

Mark D. Wilson, Gregory S. Ferguson, and George M. Whitesides*

Harvard University, Department of Chemistry Cambridge, Massachusetts 02138

Received May 22, 1989
Revised Manuscript Received November 16, 1989

The wetting of solids by liquids is dominated by short-range (van der Waals, dipolar, hydrogen bonding) interactions.[2-4] This paper examines the relationships between the wettability by water of surface-functionalized, low-density polyethylene film and the size and structures of the organic functional groups present at the solid-liquid interface. Polyethylene is a particularly instructive system, because it is a structurally heterogeneous, "nonideal" solid, in which the interfacial functional groups are disordered in both position and orientation. Its disordered structure contrasts with the more ordered self-assembled monolayers obtained by chemisorption of organic thiols on gold,[4,5] and comparisons of these systems should help to indicate the importance of interfacial order on wetting.

We have examined the wetting by water of polyethylene films having surfaces containing amide (PE-CONHR) or ester (PE-CO_2R) functionalities (**1-3**) and have determined the size of a nonpolar group R required to mask these small polar groups from contact with the water.[6] This masking doubtless reflects weakening of electrostatic and hydrogen-bonding interactions between the contacting water and the polar functional group (P).

We have described elsewhere the preparation of surface-oxidized polyethylene ("polyethylene carboxylic acid", PE-CO_2H) and the conversion of its carboxylic acid moieties to amides and esters via acid chlorides.[6-9] Here we note that (i) the functional groups

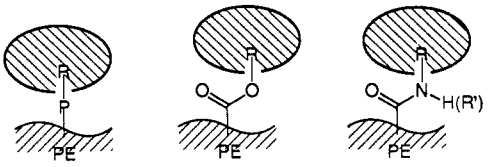

1 2 3

in these materials are restricted to a thin interfacial layer (<1-2 nm thick); (ii) approximately 30% of the organic groups present in that part of the functionalized interface that determines wetting are CO_2H groups (the remainder being methylene and ketone/aldehyde groups);[6] (iii) the conversion of CO_2H to CONHR and CO_2R groups occurs in high yields; and (iv) the interfacial region is rough and chemically heterogeneous.

The interfaces presented by PE-CO_2R and PE-CONHR to a contacting liquid are disordered, but are similar to one another in their morphologies and in their surface densities of functional groups. Figure 1 summarizes relevant measurements of advancing contact angles of water $\theta_a(H_2O)$ on these surfaces.[10] The contact angles on the interfaces having R = H (PE-CO_2H, θ_a = 55°; PE-$CONH_2$, θ_a = 43°) provide reference values. For small *n*-alkyl amides and esters (n = 1, 2), surfaces having amides are more hydrophilic than surfaces having the corresponding esters. This order—amide more wettable (hydrophilic) than ester—is in accord with other values of relative hydrophilicity such as Hansch π parameters.[11] As R increases in size through a series of *n*-alkyl groups, *n*-C_nH_{2n+1}, θ_a increases and reaches a constant value for $n \geq 6$.[12] The limiting hydrophobicities achieved by esters and amides are very similar.[13] Thus, incorporation of even small, nonpolar alkyl groups into ester or amide groups at the polyethylene-water or polyethylene-vapor interface is sufficient to shield the polar core functionality from the interactions with water

(1) This work was supported in part by the Office of Naval Research, the Defense Advanced Projects Research Agency, and the National Science Foundation under the Engineering Research Center Initiative to the Biotechnology Process Engineering Center (Cooperative Agreement CDR-88-03014). M.D.W. was an IBM Predoctoral Fellow in Polymer Science for 1986-1987. G.S.F. was a NIH Postdoctoral Fellow for 1988-1989.

(2) Israelachvili, J. *Intermolecular and Surface Forces*; Academic: London, 1985.

(3) Hugh, D. B. *Adv. Colloid Interface Sci.* **1980**, *14*, 3-41.

(4) We have previously studied wetting of oriented, self-assembled monolayer films formed by chemisorption of ω-mercapto ethers ($HS(CH_2)_{16}OR$) on gold (Bain, C. D.; Whitesides, G. M. *J. Am. Chem. Soc.* **1988**, *110*, 5897-5898). The density of polar functional groups in the interfacial region is higher for these monolayers than for PE-CO_2R. We are still defining the order in these systems. The $(CH_2)_{16}$ units seem ordered (predominantly trans extended); the R groups are significantly less ordered (Laibinis, P. E.; Nuzzo, R. G.; Whitesides, G. M. Unpublished results).

(5) Porter, M. D.; Bright, T. B.; Allara, D. L.; Chidsey, C. E. D. *J. Am. Chem. Soc.* **1987**, *109*, 3559-3568.

(6) We note, however, that the term "contact" can only be defined with respect to a given technique (e.g., measurement of contact angles) for probing the interaction. We have found previously that carboxylic acid and ester groups too deeply embedded in the polymer to be sensed by measurement of contact angles were still accessible to aqueous base (Holmes-Farley, S. R.; Whitesides, G. M. *Langmuir* **1987**, *3*, 62-76).

(7) Whitesides, G. M.; Ferguson, G. S. *Chemtracts* **1988**, *1*, 171-187.

(8) Holmes-Farley, S. R.; Whitesides, G. M. *Langmuir* **1986**, *2*, 266-281.

(9) Holmes-Farley, S. R.; Reamey, R. H.; Nuzzo, R.; McCarthy, T. J.; Whitesides, G. M. *Langmuir* **1987**, *3*, 799-815.

(10) For all esters and amides, the values of θ_a are an average of values at pH 1 (0.1 M HCl), pH 7 (0.05 M phosphate buffer), and pH 13 (0.1 M NaOH). All values reported are independent of pH. For PE-CO_2H, the value is for pH 1. These data are for sessile drops: The drop was placed on the surface by using a hypodermic needle, the drop edge allowed to advance by adding liquid, the needle withdrawn, and the contact angle measured. All measurements were made at ~100% relative humidity and room temperature. The hystereses in the angles were high (40-90°) in all cases, indicating that these systems are not at equilibrium: for further discussion on hysteresis in these systems, see ref 7.

(11) Hansch, C.; Leo, A.; Ungar, S. M.; Kim, K. H.; Nikaitani, D.; Lien, E. J. *J. Med. Chem.* **1973**, *16*, 1207-1216.

(12) For unfunctionalized polyethylene, $\theta_a \approx 103°$. The oxidation used to introduce the carboxylic acid groups in PE-CO_2H roughens the surface. This roughness is responsible for some part of the apparent hydrophobicity of the long-chain esters and amides. Another source of hydrophobicity may be the higher concentration of methyl groups near the surface of the esters and amides relative to that of PE-H (Fox, H. W.; Zisman, W. A. *J. Colloid Sci.* **1952**, *7*, 428-442).

(13) We believe that the slightly higher values of θ_a observed for the amides than for the esters reflects slightly higher yields in their formation from PE-COCl. An alternative explanation is that hydrogen bonding between the amide groups (a phenomenon that occurs in the bulk of polyurethane blends: Coleman, M. M.; Skrovanek, D. J.; Hu, J.; Painter, P. C. *Macromolecules* **1988**, *21*, 59-65) concentrates the nonpolar alkyl groups at the organic-air interface.

0002-7863/90/1512-1244$02.50/0